

Systematic Studies on Reconstruction Efficiency at Belle II

von

Martin Sobotzik

Masterarbeit in Physik
vorgelegt dem Fachbereich Physik, Mathematik und Informatik (FB 08)
der Johannes Gutenberg-Universität Mainz
am 3. Dezember 2019

1. Gutachter: Prof. Dr. Wolfgang Gradl
2. Gutachter: Prof. Dr. Habe Dünkel

Ich versichere, dass ich die Arbeit selbstständig verfasst und keine anderen als die angegebenen Quellen und Hilfsmittel benutzt sowie Zitate kenntlich gemacht habe.

Mainz, den [Datum] [Unterschrift]

Martin Sobotzik
Institut für Kernphysik
Johannes-Joachim-Becher-Weg 45
Johannes Gutenberg-Universität D-55128 Mainz
msobotzi@students.uni-mainz.de

Contents

1. Introduction	1
2. Standard Model	3
3. Experimental Setup at SuperKEKB	5
3.1. KEKB and SuperKEKB	5
3.2. The Belle II Detector	7
3.3. Coordinate System	8
3.4. Vertex detector	9
3.4.1. Pixel Vertex Detector	10
3.4.2. Silicon Vertex Detector	11
3.5. Central Drift Chamber	12
3.6. TOP and ARICH	13
3.7. Electromagnetic Calorimeter	15
3.8. K_L^0 and muon detector	16
4. Trigger and Data Acquisition System	17
5. Tools	19
5.1. Root	19
5.2. Basf2	19
6. Zusammenfassung und Ausblick	21
A. Appendix	23
A.1. Tabellen und Abbildungen	23
A.2. Weiterführende Details zur Arbeit	23
B. Danksagung	33

1. Introduction

Dieses Dokument richtet sich an Studierende am Fachbereich 08 im Studiengang Bachelor of Science (Physik). Sie finden hier Beispiele für eine mögliche Gliederung Ihrer Arbeit und Hinweise zur Strukturierung des Inhalts. Selbstverständlich sollen Sie diese Gliederung nach den Gegebenheiten Ihrer Bachelorarbeit anpassen. Besprechen Sie rechtzeitig mit Ihrem Betreuer, ob Ihr Entwurf sinnvoll ist. Holen Sie sich auch Anregungen zur Gestaltung von Abschlussarbeiten aus der Literatur ().

Sofern Sie sich dazu entscheiden, Ihr Dokument in \LaTeX zu erstellen, können Sie diese Datei als Vorlage verwenden. Fast die gesamte Literatur in der Physik verwendet \LaTeX , vor allem wegen der ausgezeichneten Möglichkeiten für das Formelschreiben.

In der Einleitung Ihrer Bachelorarbeit sollte das Thema der Arbeit möglichst allgemeinverständlich eingeführt werden. Gehen Sie dabei auch auf das weitere Umfeld der Arbeit ein und erläutern Sie, warum Aufgabenstellung und Herangehensweise interessant sind. Auch die weitere Gliederung kann angesprochen werden, um dem Leser einen ersten Überblick über den nachfolgenden Text zu geben.

2. Standard Model

	1 st	2 nd	3 rd		
Quarks	u up	c charm	t top	γ photon	H Higgs Boson
	d down	s strange	b beauty	W^{\pm} W boson	
Leptons	e electron	μ muon	τ tau	Z^0 Z boson	
	ν_e neutrino electron	ν_{μ} neutrino muon	ν_{τ} neutrino tau	g gluon	
				Gauge Bosons	

3. Experimental Setup at SuperKEKB

SuperKEKB is an two-ring, asymmetric¹, electron positron accelerator, which is located at KEK (*High Energy Accelerator Research Organization*) in Tsukuba Japan. The electron beam has an energy of 7 GeV and the positron beam has an energy of 4 GeV. These beams collide with a center-of-momentum energy of about 10.58 GeV, which is close to the mass of the $\Upsilon(4S)$ resonance. Therefore SuperKEKB is a so-called *B-factory*. The decay products are then detected by the Belle II detector to study the properties of these B mesons with high precision. In early 2018 Belle II started taking data. One goal of Belle II is to study CP-Violation with respect to new physics.[4]

3.1. KEKB and SuperKEKB

This section will only provide a rough overview of the SuperKEKB accelerator since the focus of this work is on the analysis.

SuperKEKB is an upgrade of the KEKB accelerator. KEKB was also an asymmetric electron positron accelerator in the period from 1998 to 2010, but the energies were different compared to SuperKEKB. At KEKB the electrons were accelerated to an energy of 8 GeV and the positrons to an energy of 3.5 GeV. KEKB was also a B-factory and the reaction products were then detected in the Belle detector. In 2009 KEKB achieved an instantaneous luminosity of $2.11 \cdot 10^{34} \text{ cm}^{-2} \text{ s}^{-1}$. This was the world record at that time. KEKB was discontinued after more than 10 years, to be upgraded to SuperKEKB.[1]

In figure 3.1 you can see the schematic layout of the SuperKEKB accelerator. The electrons start at the Low emittance gun. They are then accelerated in the *J*-shaped linear particle accelerator (linac). Due to lack of space, the linac has to have this special form.[3] After the curve and a second acceleration stage the electrons hit the positron production target, where the positrons are created. After this target there are more acceleration stages, before the two beams are then injected into their independent storage rings. The electrons are stored in the high-energy ring (HER) and the positrons are stored in the low-energy ring (LER). Each of these rings has a circumference of about 3 km. Both beams collide at the interaction region (IR). The products of the collisions are then detected by the Belle II detector, an upgraded version of the Belle detector.[4] (See chapter 3.2)

SuperKEKB uses a smaller asymmetry in the beam energies compared to KEKB. This allows the usage for higher beam currents and better focusing magnets. This can then result into a higher luminosity. The goal is to achieve a 40 times higher luminosity

¹asymmetric means that there is an energy difference between the two colliding beams

3. Experimental Setup at SuperKEKB

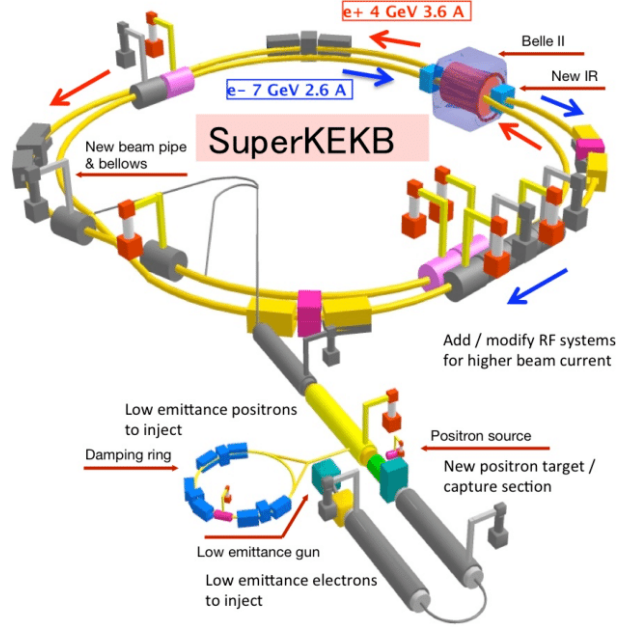


Figure 3.1.: The SuperKEKB collider.[11]

with SuperKEKB compared to KEKB. An integrated luminosity of 50 ab^{-1} will be achieved by 2025.[4]

The instantaneous luminosity \mathcal{L} specifies the performance of the collider. Knowing \mathcal{L} and the cross section σ one can calculate the events per second for a process by the following formula.

$$\frac{dN}{dt} = \mathcal{L} \cdot \sigma \quad (3.1)$$

To increase the event rate one has to increase the instantaneous luminosity since σ is given by the processes. The instantaneous luminosity can be calculate by

$$\mathcal{L} = \frac{N_{e-} N_{e+} f_c}{4\pi\sigma_x\sigma_y} \cdot S \quad (3.2)$$

assuming that both beams have a Gaussian profile of horizontal and vertical size σ_x and σ_y . In equation 3.2 N_{e-} is the number of particles in an electron bunch and N_{e+} is the number of particles in a positron bunch. f_c is the average crossing rate, which can be calculated by $f_c = n \cdot f_r$. Where n is the number of bunches and f_r is the revolution frequency. S is a reduction factor which takes geometrical effects linked to the finite cross section and bunch length into account.[15] SuperKEKB increased the luminosity by a factor of two compared to KEKB by increasing the number of bunches and the number of particles per bunch.

Also the size of the interaction region at SuperKEKB is just one twentieth of what it was at KEKB, resulting in a vertical beam size of $\sigma \approx 50 \text{ nm}$. This can be seen in

3.2. The Belle II Detector

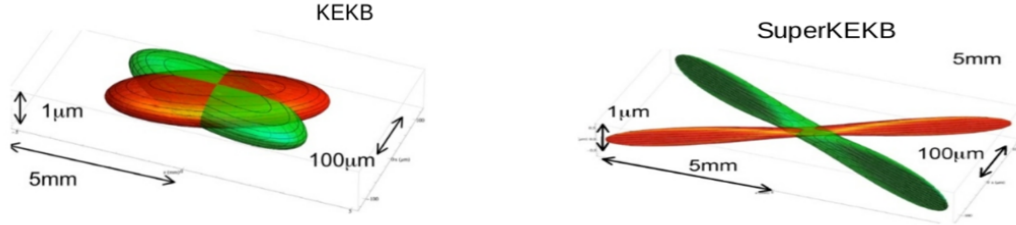


Figure 3.2.: Sketch of the beam crossing at KEKB (left) and SuperKEKB (right). At KEKB the size of the interaction region was about 10 mm. At SuperKEKB it is about 0.5 mm

figure 3.2. This decrease in beam size, along with the increase in the beam currents, it results in a overall 40-fold increase in luminosity. [2] [4]

3.2. The Belle II Detector

The Belle II detector is an upgraded version of the Belle detector which was a solid-angle magnetic spectrometer located at the interaction region of KEK. In figure 3.3 a sketch of the Belle II detector is shown. The detector contains of a variety of sub-detectors, each fulfilling a specific purpose.

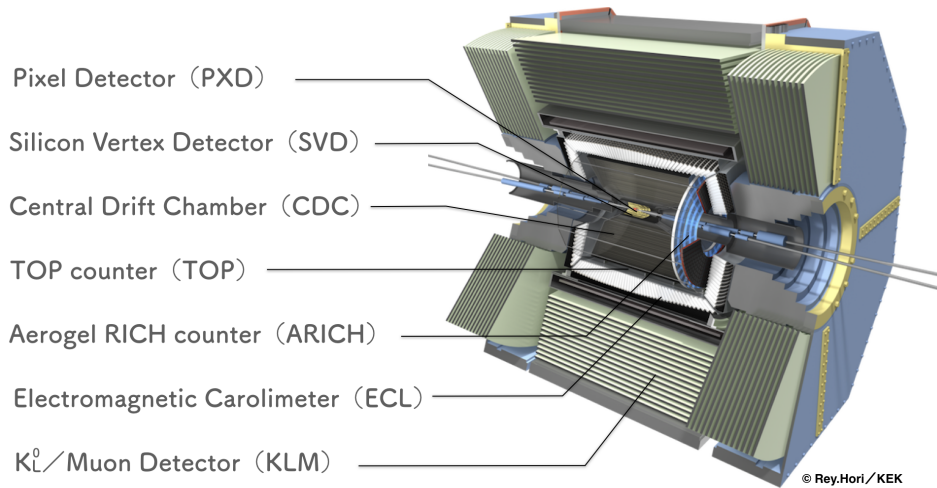


Figure 3.3.: Schematic view of the Belle II detector. The different detector elements are labeled. Also the beam pipes for the electrons and positrons with their corresponding energies are shown. [13]

In the innermost of the detector, three tracking sub-detectors are located, surrounding the IR. These sub-detectors are in a axial magnetic field of 1.5 T, provided by a

3. Experimental Setup at SuperKEKB

solenoid, to be able to reconstruct the tracks of charged particles.

The vertex detectors, consisting of the silicon vertex detector (SVD), an upgraded version of the SVD used in Belle, and the pixel detector (PXD), a new detector designed for Belle II, are used to measure the momenta of charged particles and to reconstruct decay vertices and particles with a momentum too low to reach the central drift chamber (CDC).

The CDC also already existed in the Belle detector and has been upgraded for Belle II. The CDC scans the trajectories of charged particles. From these trajectories the charge, momentum and energy loss can be determined by ionization.

These three innermost tracking detectors are surrounded by a barrel. The time-of-propagation (TOP) detector, which also got an upgrade for Belle II, surrounds the inner detectors parallel to the beam-pipes. The TOP detector, as the name suggests, measures the flight-time of charged particles. Knowing the flight-time and the momentum of the charged particles, it is possible to conclude their mass and to identify them. In the forward end-cap of the barrel are closed with an Aerogel Ring-Imaging Cerenkov detector (ARICH) which also identifies charged particles.

The next outer detector is the electromagnetic calorimeter (ECL). It surrounds all the previously mentioned detectors, and was already installed in Belle. With the ECL the energy of electromagnetically interacting particles, especially photons and electrons, can be measured.

The task of the outermost detector the K_L^0 and muon detector (KLM) is to identify K_L^0 and muons. The KLM also got upgraded for Belle II. [4]

3.3. Coordinate System

For clarification, I want to explain the coordinate system of Belle II, before I describe to the detectors in more detail.

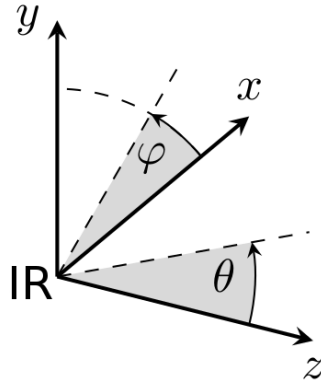


Figure 3.4.: A sketch of the coordinate system of Belle II

A sketch of the coordinate system is shown in figure 3.4. The origin of the coordinate

system corresponds to the interaction region. For the Cartesian coordinate system: The z -axis points in the direction of the magnetic field. This is also the so-called forward direction. The y -axis points up to the upper part of the detector. The x -axis points along the radial direction of the accelerator. In figure 3.4 also the spherical coordinate system is shown. Here θ corresponds to the polar angle and ϕ to the azimuthal angle.[18]

3.4. Vertex detector

The vertex detectors (VXD) is able to make precise measurements of the tracks of particles close to the interaction region. This allows the reconstruction of decay-vertices of long-lived particles. For this it is very important to determine the distance and the spatial resolution of the first measured hit, and the effect of multiple scattering.

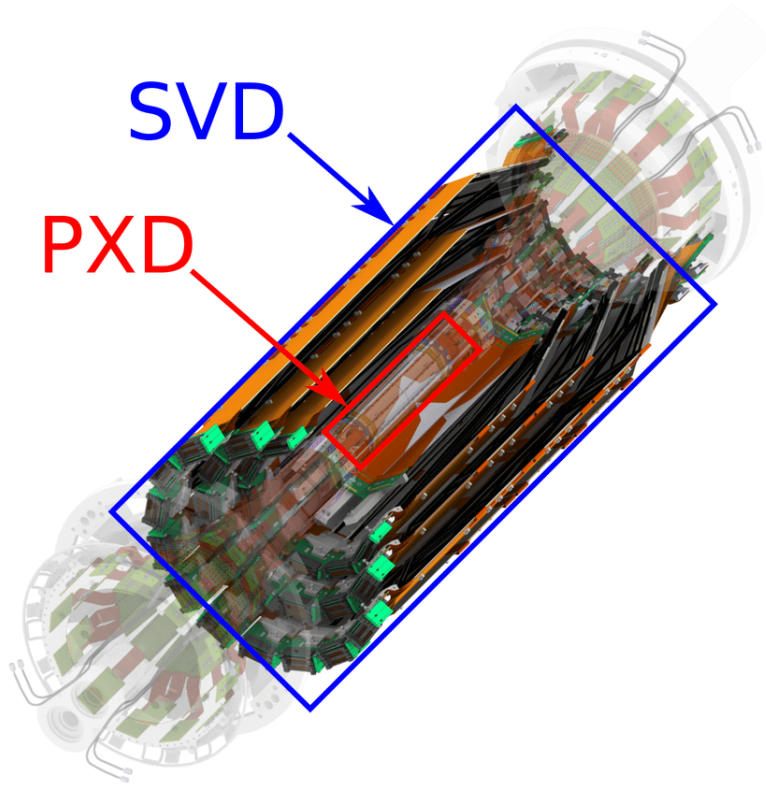


Figure 3.5.: Sketch of the vertex detectors. The vertex detector itself consists of two sub-detectors. The PXD is surrounded by the SVD. [5]

The VXD consists of the pixel vertex detector and the silicon vertex detector, both can be seen in figure 3.5. These two detectors complement each other.

3. Experimental Setup at SuperKEKB

3.4.1. Pixel Vertex Detector

The purpose of the PXD is to reconstruct the spatial position of the decay vertices of B , D and τ . The PXD is based on Depleted P-channel Field-Effect Transistor (DePFET) technology. This technology allows the sensors of the PXD to be very thin ($50\text{ }\mu\text{m}$).

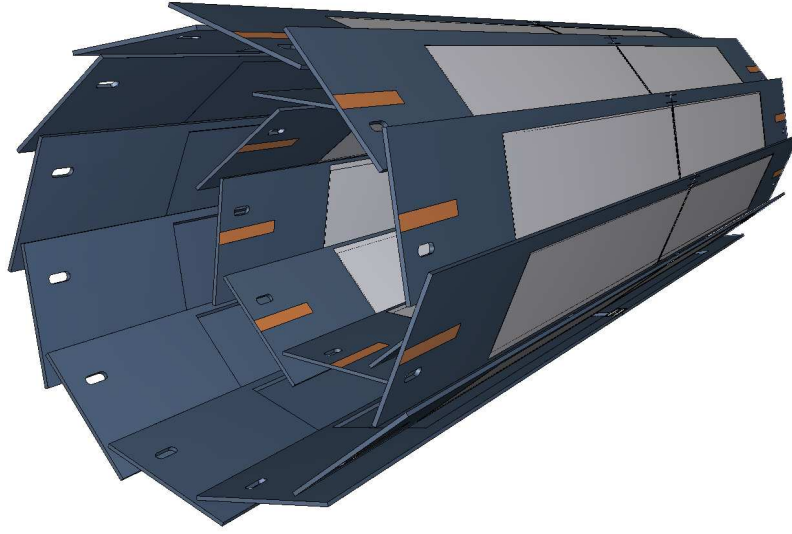


Figure 3.6.: Sketch of the PXD [2]

As you can see in figure 3.6, the PXD consists of two layers of sensors. The inner layer is made out of eight planar sensors (ladder), each has a width of 15 mm and an effective length of 90 mm. This layer has a radius of 14 mm. The second layer consists of 12 planar sensors. These sensors also have a width of 15 mm, but a length of 123 mm. The radius for the second layer is 22 mm. The PXD provides a spatial resolution of about $1.2\text{ }\mu\text{m}$. [2]

Due to the vicinity of the PXD to the interaction region, the quantum-electrodynamics background is very high, so the sensors must withstand high radiation. The DePFET technology fulfills this condition. [2] [17]

DePFET is a semiconductor detector concept invented in 1987 by J. Kemmer and G. Lutz of the MPI for Physics. This concept combines detection and amplification in one single device. [2]

A cross section of the device is shown in figure 3.7. The structure of a DePFET cell consists of fully depleted silicon. In this silicon substrate depleted by a high negative voltage a p -channel MOSFET (metal oxide semiconductor field effect transistor) or a JFET (junction field effect transistor) is integrated. The field effect transistors act as a first pre-intensification. When radiation or a particle hits the detector, electron-hole pairs are created. These pairs get separated by the potential field of the sideward

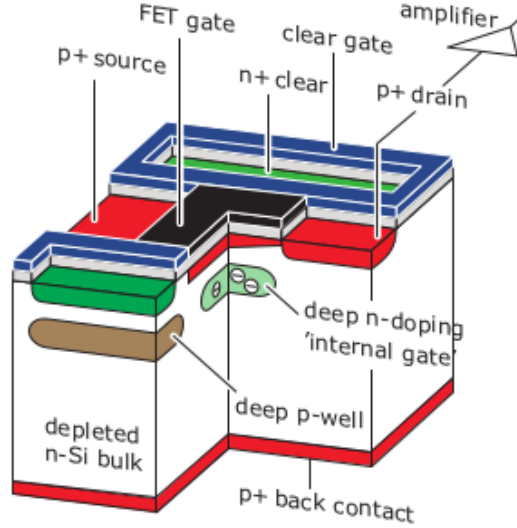


Figure 3.7.: Illustration of the DePFET technology.[2]

depletion. The positive charged holes drift to the negatively charged back contact. The negative charged electrons are collected in the potential minimum. The so-called internal gate. Above the internal gate a field emission transistor is located. The signal charged is amplified right above the position where it was generated. This avoids the leakage of lateral charge transfers. One of the most important main features of the DePFET is that the internal gate has a very small capacitance. This makes it possible to measure events affected by low noise even at room temperature.[2]

3.4.2. Silicon Vertex Detector

The SVD consists of four layers of double-sided strip detectors. The layers are located at radii of 38, 80, 115 and 140 mm. There are two different shapes of these sensors. The rectangular sensors are used in the barrel part and the trapezoidal sensors are used in the forward region of the SVD. Each sensor has a thickness of $320\text{ }\mu\text{m}$ but the sensors have different dimensions depending on the layer they are located. The barrel sensors in the most inner layer of the SVD have a dimension of $38.4 \times 122.8\text{ mm}^2$. The size for the barrel sensors of the other layers is $57.6 \times 122.8\text{ mm}^2$. The trapezoidal sensors have a dimension of 38.4 mm on the small side of the trapez to 57.6 mm on the long side of the trapez times a length of 122.8 mm.[2] An illustration of the SVD can be seen in figure 3.8.

In the barrel region the p -side of the double-sided-strip sensors is arranged parallel to the beam axis and facing the interaction region. The n -side is facing outside the detector and the n -strips are perpendicular arranged to the beam axis.

When a particles travels through the sensors it creates electron-holes pairs along its path by ionization. The electrons then propagate to the n -strips and are accumulated

3. Experimental Setup at SuperKEKB

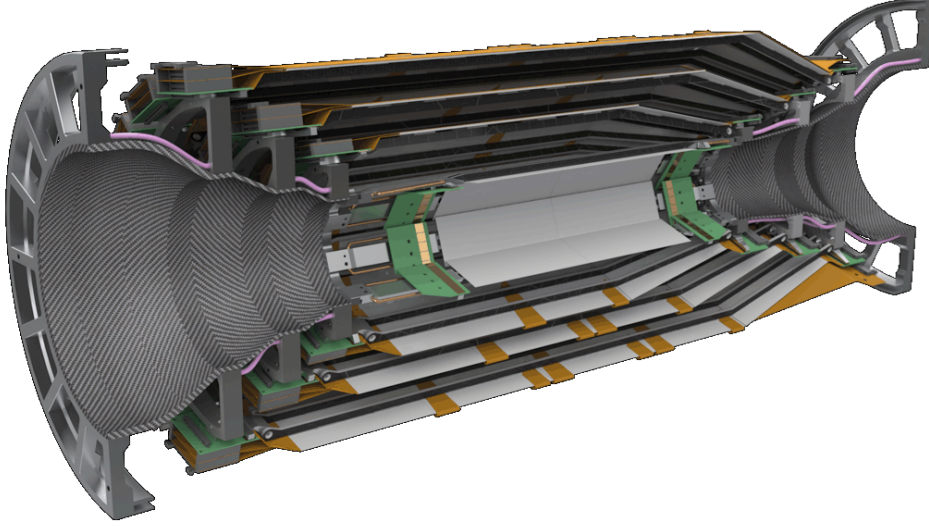


Figure 3.8.: Cross section of the silicon vertex detector[10]

there. The holes propagate to the p -strips and are collected there. The sensors then produce a signal from which the coordinate of the particle position can be read out. The p -side provides the z -direction and the n -side provides the $r - \theta$ direction.[2] [8]

3.5. Central Drift Chamber

The CDC surrounds the SVD. It consists of 14336 wires arranged in 56 layers and has an inner radius of 16 cm and an outer radius of 113 cm. The volume is filled with a 50% helium and an 50% ethane gas mixture. The purpose of the CDC is to reconstruct the momenta and tracks of charged particles, to identify these particles by measuring their specific energy loss within the gas volume. The CDC alone is able to identify low-momentum tracks, which are unable to reach the particle identification device. The CDC also acts as a reliable trigger for charged particles.[2] A small cross section of the CDC is shown in figure 3.9.

When a charged particle passes through the CDC it loses energy due to ionization of the gas. This produces electron-ion pairs, which are then separated by the electric field provided by 42240 aluminum field wires, with a diameter of $125 \mu\text{m}$. The signal is then read out by the sense wires. These have a radius of $30 \mu\text{m}$ and are made out of gold-plated tungsten.[2]

As indicated in figure 3.9 there are different superlayers in the CDC. The Dense Axial and Axial sense wires allow the reconstruction of the track in the $r - \phi$ plane. The stereo sense wires give information about the z direction. These stereo wires are tilted in respect to the z direction. Six layers of sense wires are combined to a superlayer. The CDC consists of five axial superlayers (A), and four stereo superlayer.

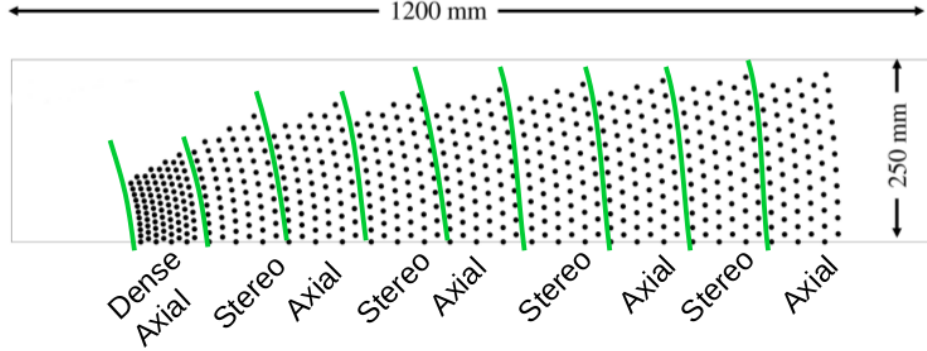


Figure 3.9.: Cross section and only a small part of the CDC. Each dot represent a wire. Also the area for the different superlayers is shown by the green line. All of these wires are immersed in a helium-ethane mixture.[14]

The four stereo superlayer subdivide into two stereo superlayer (U) with a positive stereo angle and two stereo superlayers (V) with a negative stereo angle. Starting with the innermost superlayer, every second superlayer is an axial superlayer. The stereo superlayers are between them, alternating between U and V. In total there are nine superlayers. The innermost superlayer is called *small-cell chamber* has a total of eight superlayers. (compared to the other superlayers with just six layers) This was done to lower the influence of the background, which is higher in the innermost superlayer due to the vicinity to the interaction region. The CDC has a spatial resolution of about $100 \mu\text{m}$. [2]

3.6. TOP and ARICH

There are two additional detectors for particle identification, the TOP and the ARICH. The TOP counter is located in the barrel part and it uses a combination of time-of-flight and Cerenkov angle measurements. When a charged particle with the velocity β is faster than the speed of light c_n in a medium with a reflective index n then this particle emits Cerenkov radiation under the angle θ_C . [9]

$$c_n = \frac{c_0}{n} \leq \beta \quad (3.3)$$

The Cerenkov angle is given by: [9]

$$\cos(\theta_C) = \frac{1}{n\beta} \quad (3.4)$$

Figure 3.10 shows an illustration of the functionality of a TOP bar. The charged particle emits Cerenkov light when it passes the quartz crystal. These photons then travel inside the crystal due to reflection until they are detected by a photon detector. Measuring the time difference between the emitted photons it is possible to calculate the position of the track of the charged particle. The outgoing photons are then

3. Experimental Setup at SuperKEKB

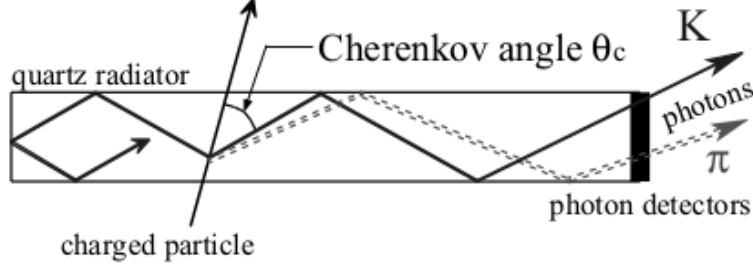


Figure 3.10.: Operating mode of a TOP detector.[2]

focused by mirrors and are then detected by PMTs. Cerenkov photons with different θ_C will be detected by different PMTs. Therefore, the TOP reconstruct the Cerenkov ring image using the information of time, x and y . [2]

The TOP counter consists of 32 quartz bars. They have a length of 1250 mm, a width of 45 mm and a depth of 20 mm. There are two quartz bars per module. The TOP counter has a K/π separation of over 99 %. [2]

The ARICH detector is located in the forward endcap region. It is designed to distinguish between kaons and pions over most of their momentum spectrum. It is also able to identify particles with a momentum below 1 GeV.

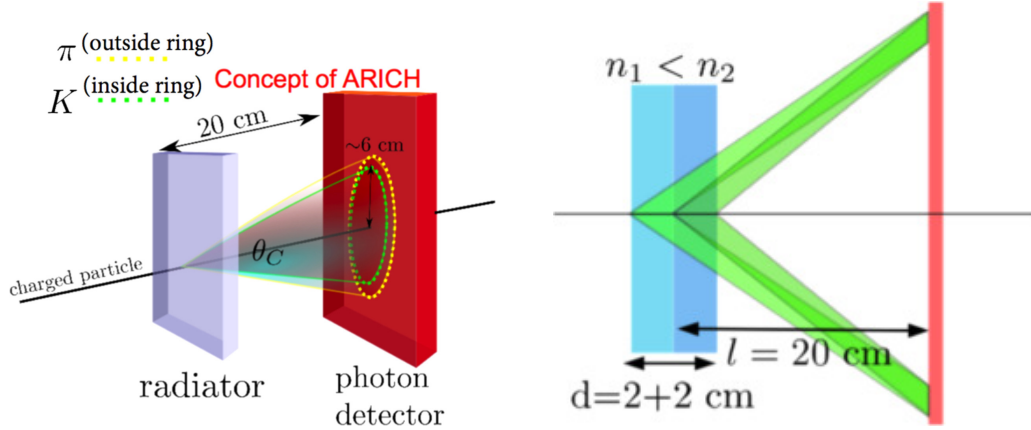


Figure 3.11.: Left: Illustration of the working principle of the ARICH detector. The yellow Cerenkov ring on the photon detector is produced by a π , the green ring by a K . Right: The radiator is shown in more detail. The radiator consists of two aerogel layers with different reflective index. [20]

In figure 3.11 the working principle of the ARICH detector is shown. A charged particle passes through two layers of an aerogel radiator with different reflective indexes and emits Cerenkov photons under an Cerenkov angle θ_C . Behind the radiator is an extension volume for the Cerenkov rings to form. At a distance of 20 cm behind the radiator is the photon detector. [2] Once the Cerenkov ring is reconstructed, the radius

of the ring can be determined and, knowing the distance and the radius, the Cerenkov angle can be calculated.

3.7. Electromagnetic Calorimeter

One of the main tasks of the ECL is the detection of photons with a high efficiency. It also determines the energy and the angular coordinates of these photons with high precision. It is also used for electron identification and the generation of a proper signal for the trigger. The ECL consists of a 3 m long barrel section with an inner radius of 1.25 m. The circular endcaps are located at a distance of $z = 1.96$ m in the forward direction and $z = -1.02$ m in the backward direction from the interaction point. The ECL covers a polar angle region of $12.4^\circ < \theta < 155.1^\circ$. Due to construction, there are two $\sim 1^\circ$ wide gaps between the barrel and the endcaps. The barrel section of the calorimeter consists of 6624 CsI(Tl)² crystals with 29 distinct shapes. Each of these crystals is a truncated pyramid with an average size of about 6×6 cm² in cross section and 30 cm in length. The length of these crystals corresponds to around 16.1 radiation lengths X_0 . The endcaps consist of 2122 CsI crystals of 69 shapes. At the end of each crystal, photo-multiplier are mounted to detect the excitation of the scintillators. The detected number of photons corresponds directly to the energy released by absorbed particles. The energy resolution of the calorimeter can be approximated as:[2] [7]

$$\frac{\sigma_E}{E} = \sqrt{\left(\frac{0.066\%}{E}\right)^2 + \left(\frac{0.81\%}{\sqrt[4]{E}}\right)^2 + (1.34\%)^2} \quad (3.5)$$

The energy E is in GeV.

Photons and electromagnetic particles are creating electromagnetic cascades when they pass through material.[16] When a high energetic photon passes through a material it creates an electron-positron pair by pair production. For this, the photon must have at least an energy of $2 \cdot m_{e^-} = 1.022$ MeV. This energy is evenly distributed between the two particles. Because these two particles are charged and their velocity changes in an the electric field of a nuclei, they generate photons through Bremsstrahlung. These processes are repeated and a electromagnetic shower is created. The energies of the particles continue to decrease until the critical energy E_c is reached. At the critical energy, the energy loss due to Bremsstrahlung is as high as the energy loss due to ionization.

If the average energy of an electron becomes E_0/e then the distance the electron traveled is called radiation length X_0 .

Assuming that the electromagnetic particles and photons interact after one radiation length and that they loose half of their energy each time they do, the total number of particles and their energy after t cascades can then be calculated by:[16]

²Thallium activated Cesium Iodide

3. Experimental Setup at SuperKEKB

$$N \simeq 2^t \quad (3.6)$$

$$E(t) \simeq \frac{E_0}{2^t} \quad (3.7)$$

This shower both spreads longitudinally and transversely. The transverse propagation can be described by the Molière radius. It can be calculated by:

$$R_M = 21 \text{ MeV} \cdot \frac{X_0}{E_c} \quad (3.8)$$

95 % of all particles of a shower are within two Molière radii.[16]

3.8. K_L^0 and muon detector

The KLM consists of an alternating sandwich structure of a 4.7 cm thick iron plates and resistive plate chambers (RPC) in between.

RPCs consist of two glass sheets, separated by a thin gas volume. These sheets act as high voltage electrodes. When a particle passes through the volume, they create ion-electron pairs which are then accelerated by the strong electric field. They therefore initiate more ionizations, which leads to a streamer between the electrodes. This causes a voltage drop in the nearby electrodes, which is detected by pick-up strips, located on both sides of the chamber. These strips are a few centimeters wide and are placed orthogonal on each side. Therefore, the particle track can be localized in z/ϕ for the barrel region and ϕ/θ for the endcaps.

To distinguish between muons and hadrons, the KLM takes advantage of the high penetration power of muons. Hadrons deplete their energy through hadronic showers in the ECL and KLM. Electrons have a shorter radiation length and are therefore absorbed by the ECL, most of the time. K_L^0 create clusters in the ECL and the KLM. These clusters are then grouped and geometrically matched to charged tracks which are detected by the inner detectors. If no corresponding charged track can be found by geometrical matching, the detected particle is then treated as K_L^0 candidate.[2][6]

4. Trigger and Data Acquisition System

5. Tools

5.1. Root

Entsprechend kann es bei einer theoretischen Arbeit sinnvoll sein, die Lösungsmethoden in einem eigenen Kapitel zu beschreiben.

5.2. Basf2

Hauptteil Ihrer Arbeit ist das Kapitel (oder die Kapitel) mit den Ergebnissen. Bei einer theoretischen Arbeit kann damit auch die Herleitung von Formeln oder die Beschreibung eines Computerprogramms gemeint sein.

6. Zusammenfassung und Ausblick

In der Zusammenfassung sollten Sie in knapper Form die Aufgabenstellung und die wichtigsten Ergebnisse rekapitulieren. Es ist für die Gutachter hilfreich, wenn Sie ausdrücklich beschreiben, worin Ihre eigenen Beiträge liegen. Scheuen Sie sich auch nicht davor auszusprechen, welche Untersuchungen durch die Zeitbegrenzung der Bachelorarbeit nicht möglich waren und nutzen Sie dies als Überleitung zu einem Ausblick auf mögliche weitergehende Arbeiten an der Aufgabenstellung.

A. Appendix

A.1. Tabellen und Abbildungen

In der Regel sind die in Tabellen und Abbildungen enthalten Informationen so wichtig, dass sie im Hauptteil der Arbeit erscheinen sollten. Unter Umständen sind aber ergänzende Tabellen und Abbildungen gut in einem Anhang aufgehoben. Wie im Hauptteil sollten Sie auch hier darauf achten, dass die in Tabellen und Figuren (siehe Abb. ??) dargestellte Information im Text angesprochen wird und selbsterklärende Legenden vorhanden sind.

A.2. Weiterführende Details zur Arbeit

Manch wichtiger Teil Ihrer tatsächlichen Arbeit ist zu technisch und würde den Hauptteil des Textes unübersichtlich machen, beispielsweise wenn es um die Details des Versuchsaufbaus in einer experimentellen Arbeit oder um den für eine numerische Auswertung verwendeten Algorithmus geht. Dennoch ist es sinnvoll, entsprechende Beschreibungen in einem Anhang Ihrer Bachelorarbeit aufzunehmen. Insbesondere für zukünftige Arbeiten, die an Ihre Bachelorarbeit anschließen, sind dies manchmal hilfreiche Informationen.

List of Figures

3.1. SuperKEKB Collider	6
3.2. Sketch of the Beam Crossing for KEKB and SuperKEKB	7
3.3. Belle II Detector	7
3.4. Coordinate System of Belle II	8
3.5. Vertex Detector	9
3.6. Pixel Detector	10
3.7. DePFET	11
3.8. Silicon Vertex Detector	12
3.9. Central Drift Chamber	13
3.10. TOP Principle	14
3.11. ARICH	14

List of Tables

Machen Sie genaue Angaben, so dass die verwendeten Literaturstellen eindeutig identifiziert und aufgefunden werden können. Bei Lehrbüchern ist es sinnvoll, den Titel anzugeben, eventuell auch die Ausgabe. Bei Artikeln in Fachzeitschriften ist es üblich, nur die gebräuchlichen Abkürzungen für den Titel der Zeitschrift, Band, Erscheinungsjahr und Seite anzugeben. Unter Umständen kann es auch sinnvoll sein, im Internet aufgefundene Informationsquellen anzugeben, zum Beispiel für Software oder zu den Details von Ergebnissen großer experimenteller Kollaborationen. Es ist selbstverständlich, dass Sie auch Bachelor, Diplom- oder Doktorarbeiten angeben, wenn Sie diese in Ihrer eigenen Arbeit verwendet haben.

Im folgenden Beispiel werden die in der Datei enthaltenen Anweisungen als Stilvorlage verwendet. Andere Möglichkeiten für die Gestaltung eines Literaturverzeichnisses findet man im Internet: <http://janeden.net/bibliographien-mit-latex>.

Bibliography

- [1] Abe et al.
“Achievements of KEKB”.
In: *Progress of Theoretical and Experimental Physics* 2013.3 (Mar. 2013).
ISSN: 2050-3911.
DOI: 10.1093/ptep/pts102.
eprint: <http://oup.prod.sis.lan/ptep/article-pdf/2013/3/03A001/4440618/pts102.pdf>.
URL: <https://dx.doi.org/10.1093/ptep/pts102>.
- [2] Abe et al.
“Belle II Technical Design Report”.
In: (Nov. 2010).
URL: [arXiv:1011.0352](https://arxiv.org/abs/1011.0352).
- [3] Akemoto et al.
“The KEKB injector linac”.
In: *Progress of Theoretical and Experimental Physics* 2013.3 (Mar. 2013).
ISSN: 2050-3911.
DOI: 10.1093/ptep/ptt011.
eprint: <http://oup.prod.sis.lan/ptep/article-pdf/2013/3/03A002/4441335/ptt011.pdf>.
URL: <https://dx.doi.org/10.1093/ptep/ptt011>.
- [4] E. Kou et al.
The Belle II Physics Book.
Aug. 2018.
URL: <https://arxiv.org/abs/1808.10567>.
- [5] F. Bernlochner et al.
“Online Data Reduction for the Belle II Experiment using DATCON”.
In: (Sept. 2017).
DOI: 10.1051/epjconf/201715000014.
URL: <https://arxiv.org/abs/1709.00612>.
- [6] T. Aushev et al.
“A scintillator based endcap K L and muon detector for the Belle II experiment”.
In: (Apr. 2015).
DOI: 10.1016/j.nima.2015.03.060.
URL: <https://arxiv.org/abs/1406.3267v3>.
- [7] V. Aulchenko et al.

Bibliography

- “Electromagnetic calorimeter for Belle II”.
In: *Journal of Physics: Conference Series* 587 (2015), p. 012045.
DOI: 10.1088/1742-6596/587/1/012045.
URL: <https://doi.org/10.1088/1742-6596/587/1/012045>.
- [8] Thomas Bergauer.
“The silicon vertex detector of the Belle II experiment”.
In: *PoS* (2010), p. 044.
- [9] PA Cerenkov.
“PA Cerenkov, Phys. Rev. 52, 378 (1937).”
In: *Phys. Rev.* 52 (1937), p. 378.
- [10] Belle II Italian collaboration.
Silicon Vertex Detector.
Mar. 2019.
URL: <https://web.infn.it/Belle-II/index.php/detector/svd>.
visited on 06.03.2019.
- [11] Ivan Heredia de la Cruz.
“The Belle II experiment: fundamental physics at the flavor frontier”.
In: *Journal of Physics: Conference Series* 761 (Sept. 2016).
DOI: 10.1088/1742-6596/761/1/012017.
- [12] Filippo Dattola, Lorenzo Vitale, and Diego Tonelli.
“Tracking studies for the Belle II detector”.
Presented on 20 07 2018.
PhD thesis. Trieste: Trieste, University of Trieste, 2018.
- [13] *Electrons and Positrons Collide for the first time in the SuperKEKB Accelerator*.
Apr. 2018.
URL: <https://www.kek.jp/en/newsroom/2018/04/26/0700/>.
visited on 25.02.2019.
- [14] Thomas Haut. *Pattern Recognition at Belle II*.
Dec. 2016.
- [15] Werner Herr and Bruno Muratori.
“Concept of luminosity”.
In: (Feb. 2006).
DOI: 10.5170/CERN-2006-002.361.
- [16] William R Leo.
Techniques for nuclear and particle physics experiments: a how-to approach.
Springer Science & Business Media, 2012.
DOI: 10.1007/978-3-642-57920-2.
- [17] C. Marinas and M. Vos.
“The Belle-II DEPFET pixel detector: A step forward in vertexing in the superKEKB flavour factory”.

- In: *Nuclear Instruments and Methods in Physics Research Section A: Accelerators, Spectrometers, Detectors and Associated Equipment* 650.1 (2011). International Workshop on Semiconductor Pixel Detectors for Particles and Imaging 2010, pp. 59 –63.
ISSN: 0168-9002.
DOI: <https://doi.org/10.1016/j.nima.2010.12.116>.
URL: <http://www.sciencedirect.com/science/article/pii/S0168900210028962>.
- [18] Nobuhiro Shimizu.
“Development of the Silicon Vertex Detector for Belle II experiment”.
Department of Physics, University of Tokyo.
URL: http://hep.phys.s.u-tokyo.ac.jp/?page_id=229.
visited on 25.02.2019.
- [19] *Standard Model*.
URL: <https://www.physik.uzh.ch/en/researcharea/lhcb/outreach/StandardModel.html>.
visited on 19.03.2019.
- [20] E. Torassa.
“Particle identification with the TOP and ARICH detectors at Belle II”.
In: *Nuclear Instruments and Methods in Physics Research Section A: Accelerators, Spectrometers, Detectors and Associated Equipment* 824 (2016). Frontier Detectors for Frontier Physics: Proceedings of the 13th Pisa Meeting on Advanced Detectors, pp. 152 –155.
ISSN: 0168-9002.
DOI: <https://doi.org/10.1016/j.nima.2015.11.016>.
URL: <http://www.sciencedirect.com/science/article/pii/S0168900215013789>.

B. Danksagung

... an wen auch immer. Denken Sie an Ihre Freundinnen und Freunde, Familie, Lehrer, Berater und Kollegen.